Tallá Ferrer, C.; Vilariño, G.; Rizk, M.; Sydow, H.; Vallés Lluch, A. (2020). Nanocomposites based on poly(glycerol sebacate) with silica nanoparticles with potential application in dental tissue engineering. International Journal of Polymeric Materials. 69(12):761-772. https://doi.org/10.1080/00914037.2019.1616197

NANOCOMPOSITES BASED ON POLY(GLYCEROL SEBACATE) WITH SILICA NANOPARTICLES WITH POTENTIAL APPLICATION IN DENTAL TISSUE ENGINEERING

C. Tallá Ferrer[1], G. Vilariño-Feltrer[1], M. Rizk[2], H.G. Sydow[3], A. Vallés-Lluch[1,4,*]

[1] Centre for Biomaterials and Tissue Engineering, Universitat Politècnica de València, Spain

[2] Department for Preventive Dentistry, Parodontology and Cariology, University Medical Center Göttingen, Germany

[3] Institute of Anatomy and Embryology, University Medical Center, Göttingen, Germany

[4] Biomedical Research Networking Centre in Bioengineering, Biomaterials and Nanomedicine (CIBER-BBN), Spain

** Corresponding author. E-mail address: avalles@ter.upv.es*

Abstract

Nanocomposites based on poly(glycerol sebacate) with silica nanoparticles were synthesized to explore their potential use in the biomedical field. The nanoparticles were two distinct polyhedral oligomeric silsesquioxanes (POSS), both used at 5% wt/wt concentration, specifically methacrylisobutyl POSS and methacryl POSS. These materials were investigated for their possible application as coatings as well as with regenerative purposes in dental engineering, and their viability for this application was assessed. Thus, pure PGS and nanohybrids thereof were obtained as scaffolds (that is, porous structures, designed with regenerative purposes) and as films (intended for coatings and to be used as controls).

Keywords: poly(glycerol sebacate); POSS; elastomer; nanocomposite; hydroxyapatite

1. INTRODUCTION

Poly(glycerol sebacate), PGS, is a synthetic elastomeric polymer recently discovered. It was firstly described by Wang *et al.* [1], as a new elastomer that forms a covalently crosslinked and three-dimensional network of random coils with hydroxyl groups linked to its backbone. This polymer is biodegradable, has shown a good biocompatibility and is much tougher than most hydrogels, the most common crosslinked biomaterials [1].

PGS is formed by the polycondensation reaction of glycerol and sebacic acid, both non-toxic components [1-3]. Glycerol is a building block for lipids used in pharmaceutical industry and is approved by the Food and Drug Administration (FDA). Sebacic acid is the natural intermediate in ω-oxidation of medium-to-long-chain fatty acids and is also approved by the FDA for drug delivery applications [4]. The reaction is conventionally carried out in two steps: (1) pre-polymerization, resulting in a viscous pre-polymer by formation of linear chains between reacting monomers (hereinafter called pre-PGS) and (2) curing or crosslinking step, in which the chains intertwine yielding the polymer network.

This polymer has been recently explored in the tissue engineering field because of its interesting properties. Beside biodegradable, it is a non-toxic material with elastomeric properties, relatively inexpensive and no solvents or catalysts are needed for its synthesis. These characteristics make the PGS highly interesting for biomedical applications. So far, PGS is becoming important for soft tissues: some of the applications proposed for this polymer are skin regeneration [5], cardiac tissue [6] and corneal stroma [7]. Nonetheless, it has also been proposed to regenerate hard tissues [8]. Other applications for PGS are in drug and gene delivery [2], but PGS can also be used as a surgical glue [9].

With the aim of improving the properties of a given polymer, hybrid materials that combine polymeric materials with other component/s have been largely proposed in the literature. In particular, nanomaterials such as clay-layered silicates, single and multi-walled nanotubes, carbon nanofibers and polyhedral oligomeric silesquioxane (POSS) nanostructured compounds have shown to be promising materials to combine with polymeric matrices [10-13]. Silesquioxanes are structures that follow the formula $RSiO_{1.5}$, where R refers to hydrogen, or alkyl, alkylene, aryl and arylene groups and the organofunctional derivates of them. The first oligomeric organosilsesquioxanes, $(CH_3SiO_{1.5})_n$ were found by D.W. Scott in 1946 through thermolysis of polymeric products from methyltrichlorosilane and dimethylchlorosilane cohydrolisys [14]. POSS nanostructured chemicals have sizes of 1 to 3 nm in diameter, but they have the ability to build higher dimensionality compounds by aggregation or crystallization of POSS macromers and a polymer [15, 16].

The interest of incorporating POSS particles into a polymeric matrix can be attributed to the enhancement of mechanical properties and the combination of compatibility and chemical stability because of its inorganic-organic architecture: POSS molecule contains organic substituents on its outer surface that make it compatible with polymers or biological systems [15, 16]. Some POSS/polymer materials have been proposed for tissue engineering and used in first-in-human applications. As an example, Jungebluth *et al.* [17] did a tracheobronchial transplantation with a tailored trachea made of poly-(carbonate-urea) urethane (PCU) and POSS, and seeded stem cells on it. Also, Nayyer *et al.* [18] manufactured a nanocomposite POSS/PCU auricular scaffold that had more similar elastic modulus to ear cartilage than some of the currently used compounds, and observed that it supported fibroblast ingrowth and proliferation. Moreover, the POSS

particles could favour the nucleation of hydroxyapatite on the surface of the nanocomposite. This ability, which could be described as bioactivity, is interesting for hard tissues and specifically in dental applications.

Thus, the main objective of this work was to explore the potential of biomaterials based on PGS, modified by two different POSS nanoparticles. These engineered biomaterials are proposed for their use in the odontology field as coatings of devices of diverse type (metal fixing screws for example) or as scaffolds with regenerative purposes. With the purpose of studying their viability for these applications and ultimately comparing their performance, PGS and its nanocomposites were synthesized as bulk films and porous materials (scaffolds). To obtain the scaffolds, a solvent casting-polymerization in a porogen template-particulate leaching technique was followed; this procedure was previously set [19] and adapted herein for the incorporation of the nanoparticles.

2. MATERIALS AND METHODS

Preparation of PGS films and scaffolds

Synthesis of poly(glycerol sebacate) was carried out in two stages: an initial pre-polymerization, which results in the formation of linear chains between the monomers, glycerol (VWR International) and sebacic acid (Sigma-Aldrich), and a second or curing step, when crosslinks between these chains occur and a percolated polymeric network is obtained. The pre-polymerization reaction was performed with equimolar proportions of sebacic acid and glycerol during 24 h at 130ºC in a three-neck round-bottom flask, inert atmosphere (N_2) and stirring, as described in [20]. The inert atmosphere was achieved by

a continuous nitrogen gas flow connected to a nitrogen trap that allowed nitrogen to escape but limited the inlet of air. Previously, the thermoregulated magnetic stirrer (Arex VELP Scientifica) was connected and set at 140ºC to melt the sebacic acid, and following the temperature was set at 130ºC with stirring at 100-150 rpm up to 24 h (taking into account also the time of stirring at 140ºC).

After this point, the pre-PGS was divided in three parts, in order to get three different types of samples: one was pure pre-PGS, in the second batch 5% wt/wt of methacrylisobutyl POSS (943.64 gr/mol, Hybrid Plastic) with one functional group was added (hereinafter referred to as POSS1), and in the third 5% wt/wt of metacryl POSS cage mixture (1433.97 gr/mol, Hybrid Plastic) with 8 functional groups was incorporated (hereinafter referred to as POSS8). POSS particles were added always after the pre-polymerization, and the pre-PGS/particles mixture was stirred *ca*. 30 min, until a good dispersion was observed.

For the curing of the films, each pre-polymer (pure or with nanoparticles) was poured in a mould with dimensions of 3 x 3.3 cm, 1 mm-thick. Each mould was previously prepared with a Teflon sheet and a glass plaque covered with adhesive plastic. The filled moulds were placed in a vacuum heater (Vacuo-Temp SELECTA) at 130ºC during 48 h, followed by demoulding.

For the scaffolds, the curing was done in a drilled Teflon mould (holes of 7 mm in diameter, 10 mm high) filled with a porogen bed made of sodium chloride, as described in [19]. Briefly, the porogen bed was obtained by a salt fusion method, which takes advantage of humidity for the surface dissolution of the salt granules, and its fusion under the effect of pressure, to yield a porogen template. This procedure was firstly described

in PGS by Gao *et al*. [21]. In this study sodium chloride of 212-215 μm in diameter was used, introduced in a drilled Teflon mould, and compacted using glass rods.

Pre-PGS and pre-PGS/POSS mixtures were injected in the templates at a pre-polymer/porogen weight ratio of 1/9, which was found in [19] to provide the best biological results. The moulds were kept at 130ºC under vacuum for 48 h to allow the PGS to cure, followed by demoulding.

Rinsing

Films were immersed in 60 mL of ethanol (Scharlau) each for 24 h on an orbital stirrer at 100 rpm. Next, the ethanol was renewed and the films remained immersed another 24 h. After that, the films were moved to deionized water. The water replacement was progressive to avoid the fracture of the films. The films stayed in water 48 h with a change at 24 h.

The scaffolds had to be previously rinsed, so the cured templates, cut into slices 1 mm high, were immersed during 2 days in deionized water (Mili-Q) at room temperature, 50 mL per scaffold, as described in [19]. After that, the rinsing procedure was analogous to that of the films.

Viscosity Analysis of pre-PGS

In order to characterize the polymerization of PGS, viscosity analyses were performed following the reaction, starting from the monomers. For this purpose, equimolar proportions of sebacic and glycerol were poured in a round-bottom flask. The mixture was heated up to 140ºC to melt the sebacic acid. When melted, the flask was settled at 130ºC and the mixture was stirred for 30 min.

The mixture was placed next in a rheometer (AR-200ex, TA instruments), and a velocity of the moving plate of 1.5 rad/s was applied during 72 h at a constant temperature of 130ºC. The geometries used were 25 mm-diameter parallel aluminium plates.

Fourier-Transform Infrared Analysis of the films

Attenuated total reflectance Fourier-transform infrared (ATR-FTIR) spectra were obtained for the films with different compositions in a TENSOR II FTIR spectrometer (Bruker). These measurements allowed studying the homogeneity of the distribution of inorganic particles and explore the plausibility of hybrid bonds between PGS and POSS. Absorbance was measured between 700 and 4000 cm^{-1} and the resulting spectra was the average of 32 scans with a resolution of 4 cm^{-1}.

Morphological analysis by Scanning Electron Microscopy and Energy Dispersive X-ray Spectroscopy

Films and scaffolds of each composition were sputtered with carbon and observed under Field Emission Scanning Electron Microscopy (FESEM) at 5 kV, and a silicon reference was measured first. An ULTRA 55 ZEISS microscope was used, equipped with a secondary electron detector, backscattered electron detector and an X-Ray Dispersive Energy Detector (EDS) to obtain images of the samples surface and a qualitative and quantitative analysis of their composition and distribution of elements.

Porous morphology and pore analysis of the scaffolds by Microcomputed Tomography

Microcomputed tomography (MicroCT) was used to non-invasively study the morphology of the scaffolds. The scanner used for the measurements was a Skyscan-1272 from Bruker. The size of each sample observed was around 1 cm high (as obtained, before

cutting it into slices) and 7 mm in diameter. The measurement conditions were: 40 kV, 212 µA, resolution 1632x1092, pixel size of 5 microns, exposure time 511 ms and rotation step of 0.6 degrees. The settings for short measurements (8 min) were chosen to avoid otherwise very strong artefacts originating from the slow expansion and movement of the foamy samples. Due to the very low density of the samples no filter was used for the measurements. The obtained data were reconstructed using NRecon with beam-hardening corrections of 0%, ring artefact corrections ranging from 0 to 10 and the volumetric and structural analysis were performed using CTan software.

Thermogravimetric Analysis and Differential Scanning Calorimetry

Thermogravimetric analysis (TGA) was performed with a TGA/DSC 2 STAR System (Mettler Toledo). The three types of films were scanned, as well as pure POSS particles, to analyse their specific profile. The actual (experimental) percentage of nanoparticles in the hybrids (after rinsing the samples) was quantified from the data of the residues by comparison with the nominal (theoretical) one. The degradation curves allowed studying the influence of the nanoparticles on the thermal behaviour of PGS. Platinum pans of 70 µl were used and approximately 5 mg of each material were weighed for each test. The experiments were performed from 30ºC to 800ºC at $10ºC \cdot min^{-1}$ under nitrogen atmosphere, with a flow rate of $50\ ml \cdot min^{-1}$.

Differential Scanning Calorimetry (DSC) measurements were performed with the three types of films in order to characterize their thermal properties in the glass transition and melting processes. The analysis was performed with a Perkin-Elmer DSC 8000. Aluminium sample pans of 100 µl were used. Each sample consisted of approximately 5 mg of material. The pans were cooled to -80ºC and stabilized for 2 min, next heated at

20ºC·min^{-1} and scanned up to 60ºC. Measurements were performed under nitrogen atmosphere.

Density and swelling

Density of the films was measured with a Mettler AX205 (Mettler Toledo) balance, equipped with a Mettler ME 33360 density accessory kit, through Archimedes' principle. The samples were weighed dry, m, and after immersion in n-octane, m_i, (Sigma Aldrich, 98% purity, $\rho_{n\text{-}octane}$=0.703 gcm^{-3}), which is a non-solvent and thus does not cause the swelling of the matrices. Three replicates of PGS, PGS/POSS1 and PGS/POSS8 were measured. Each replicate was approximately 0.6x0.5x0.2 cm^3. The density, ρ, was calculated from the weight of the sample in air, divided by the volume of n-octane displaced, V_{dis}:

$$\rho = \frac{m}{V_{dis}} = \frac{m}{(m - m_i)/\rho_{n-octane}}$$

On the other hand, the swelling of the films was quantified at equilibrium (constant mass), also with three replicates per type of sample and swelling medium, having a size of 0.6x0.5x0.2 cm^3. The measurements were performed by weighing the samples in a dry state, and after immersion in three different media at 37ºC: artificial saliva (AS), prepared as in [22], deionized water with its pH adjusted to that of artificial saliva, pH = 6.4, and cell culture media: Dulbecco's Modified Eagle Medium with Glutamax (Fisher), low glucose and pyruvate with 10% v/v fetal bovine serum, 1% v/v penicillin streptomycin and 0.02% v/v sodium azide (99.5%, ReagentPlus®).

Mechanical analysis

Compression tests were performed to analyse and compare the mechanical properties of the scaffolds and films. A Seiko TMA SS6000 dilatometer was used with a 3 mm diameter rod. The rod applied a progressive compression force from 0 to 1500 mN with a rate of 100 mN/min. The tests were performed at 37±2 ºC with the samples immersed in artificial saliva in order to simulate physiological conditions. 5 replicates per scaffold composition and 3 per film were scanned. The scaffolds were cut from the starting cylinders with a thickness of 1.5-2 mm, and the films were cut as squares of 4x 4 mm^2, and their thickness was approx. 1.5 mm as well. Parallel surfaces were ensured in all cases.

From the stress-strain curves obtained, the Young modulus (E) of each sample tested was calculated using the initial slope. More specifically, two moduli could be obtained for the scaffolds, at low deformations (E_1) -the initial slope of the stress-strain curves up to 20 kPa- and at stresses above 60 kPa (E_2). The Young's moduli of the films were measured at stresses between 60 and 100 kPa.

Degradation

In order to assess the weight loss of the materials by hydrolysis in physiological media, a degradation experiment was performed up to 4 weeks. This final time was chosen based on related works in which mass loss of PGS nanocomposites was followed during 4 days (PGS combined with silica bioactive glass) [23], 28 days (with nano-fumed silica) [24], or 2 months (with 45S5 Bioglass® particles) [25]. 4 replicates per type of scaffold were immersed in 2 ml of artificial saliva each and, in parallel, an analogous experiment was followed in deionized water with the pH adjusted to 6.4. The replicates had a size of

approximately 0.5x0.3 mm^2 and were weighed dry before the experiment. Next, they were placed in Eppendorf tubes with their corresponding media, and incubated at 37ºC. After 4 weeks the samples were withdrawn, dried and weighed again.

Bioactivity test

The study of nucleation of hydroxyapatite (HAp) on the surface was carried out with the scaffolds, 2 replicates per type, following the procedure described by Kokubo [26]. Samples were immersed in artificial saliva (as a simulated body fluid) to lengthen the time points to 2 weeks, 3 weeks and 4 weeks. Afterwards, the samples were dried and analysed by MicroCT, EDX (FEI QUANTA 200F, SEM-EDX at 12.5 Kv) and FESEM (ULTRA PLUS ZEISS).

Cell viability test

In order to ascertain the biocompatibility of the materials, a cytotoxicity test was done using L-929 fibroblasts (from the DSMZ No. ACC 2 in Braunschweig -German Collection of Microorganisms and Cell Cultures: Human and Animal Cell Cultures). PGS-based scaffolds and films were cultured and analyzed, 3 replicates per type and 3 cell viability tests per experiment. The scaffolds were cut as disks 2 mm-thick, 5-7 mm in diameter. The films were cut as 5x5x2 mm^3.

To sanitize samples, they were soaked for 1 h in vials with 70% ethanol, and next transferred to new well culture plates to be progressively soaked in 70, 50, 30% ethanol and pure MiliQ water (10 min in each). Samples were then kept until cell seeding in culture medium in an incubator at 37ºC, 5% CO_2. All the tests were performed in P48 multi-well plates. As positive control (cytotoxic) fragments of latex were used and the

media with the cells was used as negative control (non-cytotoxic). An extra sample in each case lodged in the multi-well plate served as blank.

The seeding was performed by filling the wells with 500 µl of DMEM medium, containing $2x10^4$ cells. The plate was next incubated at 37ºC and 5% CO_2. After 48 h in the incubator, the medium was withdrawn. To determine cell viability, a Cell Counting Kit-8 (CCK-8; Dojindo) was used. The solution of CCK8 and medium was poured in each well (270 µl of DMEM and 30 µl of CCK8). After 2 h of incubation, the absorbance was measured at 450 nm and 650 nm in a multi-detection microplate reader SPECTRAmax M2 spectrophotometer with dual-mode and compared to the blank.

Statistics

Experimental data are given as mean ± standard deviation, and statistical assessment was done for density, swelling, compression and degradation tests, with Statgraphics Centurion XVI.II software (Statgraphics Technologies). Variance analysis and multiple range comparison tests were calculated at 95% significance level ($p < 0.05$) to determine the significance of the differences observed in the results of the different experiments. The selected method for the comparisons was the Fisher's least significant difference (LSD) test (similarity of sample variances was statistically assessed).

3. RESULTS AND DISCUSSION

Characterization of the reaction between glycerol and sebacic acid

The viscosity variation with reaction time is shown in Figure 1. There is a first stage where the viscosity smoothly increases as the pre-polymerization occurs, and oligomers as well as branched long chains are formed starting from the monomers. Then, the crosslinks between isolated intermediate species allow the percolation of the network at around 40 h, revealed by a significant increase of its viscosity.

The initial viscosity of the monomers mixture was 0.015 Pa·s, and after 51.41 hours at 130ºC the reacting mixture had a maximum viscosity of 652.086 Pa·s. This means that PGS has more than 40000 times the viscosity of its monomers because of the formation of longer branched chains and their crosslink and percolation. Also, theoretical lines were drawn following the trend of the pre-polymerization step (from 0 to 40 h) and of the curing (45 h to 51 h). The intersection between these two lines gives the gel point: this viscosity is around 0.500 Pa·s and occurs at 46.7 h, which means that during the first step the viscosity increases 30 times and during the curing it does so more than 1300 times.

Chemical analysis and nanoparticles distribution

Infrared spectroscopy was used to qualitatively analyze the functional groups present in each hybrid and explore the presence of hybrid bonds, and, thus, to compare the influence of the nanoparticles tested.

The FTIR spectra (Figure 2) show that PGS and PGS/POSS1 have similar profile, whereas the material with POSS8 particles differs at lower wavelengths: in the PGS/POSS8 sample a strong peak appears at 1100 cm^{-1}, which could be interpreted as Si-

O-Si bonds present in the POSS particles or Si-O-C bonds [27]. This band is characteristic of POSS particles [28,29], its intensity increasing with its content [29]. This latter bond could be that between the inorganic moieties of the POSS particle with the organic functionalization, but also could be indicative of a hybrid bonding with the polymer (PGS). Further experiments would be required to confirm this.

For all samples there is a broad band between 3600 and 3200 cm^{-1} characteristic of OH groups. Two peaks appear at 2927 cm^{-1} and 2857 cm^{-1} belonging to CH_x and the strong peak at 1730 cm^{-1} corresponds to C=O of carboxyl or condensed ester groups. The results are similar to those found in the literature for PGS [20,30]. However, in PGS/POSS8 samples, the intensity of the peaks belonging to these groups is lower in comparison with the other two; this could be attributed to a greater PGS crosslinking in the presence of POSS8 particles, which will be analysed later.

On the other hand, elemental analysis allowed to determine the presence of silicon particles at surface level and section, as well as their distribution. In Figure 3 images of the surfaces with particles are shown, together with the maps of silicon element resulting from the EDS lecture, as red dots. They show the uniform presence of silicon, indicating the homogeneous distribution of the nanoparticles.

In films with POSS1 the highest values of silicon were observed at the surface level of the samples (between 1 and 3 wt%), whereas in PGS/POSS8 films there was more silicon in the sections (~10 wt%). These results suggest that POSS8 particles are better dispersed than POSS1 particles, which in turn remain preferably at the surface level.

The different dispersion of the particles could be a result of their state. Indeed, POSS1 particles are a white powder, whilst POSS8 is a viscous liquid at room temperature, so it

was easier to get a homogenous mixture with the latter, and were finally much better distributed within the polymer network. On the other hand, the higher presence of POSS1 particles at the surface could be due to the vacuum applied during the curing. POSS1 particles are lighter, so when vacuum is applied they diffuse towards the surface. An effect of the rinsing cannot be excluded, since samples swell in ethanol and a fraction of particles can also diffuse and be rinsed. This could happen also with POSS8 particles, since they are soluble in ethanol, obviously, but in any case the EDS images and quantitative data clearly show that there are more Si-based particles in the PGS/POSS8 films, better dispersed and entrapped in the polymeric matrix.

Structure and pore analysis of the scaffolds

Obtaining PGS-based nanocomposites with POSS particles is feasible, and also to design them as sponge-like scaffolds with interconnected pores by particulate leaching. After removing the porogen salt and drying, scaffolds had the appearance of foam (Figure 4). The dimensions of the scaffolds were more or less those of the mould (10 mm-high and 7 mm in diameter, before slicing). The architectural analysis (pore size and pore distribution) was done by microcomputed tomography, and then the porosity of the materials (volume fraction of pores) was quantified using the CTanalyser software. For pure PGS scaffolds the obtained porosity was 38.7±5.2%, whereas for PGS/POSS1 and PGS/POSS8 it was 36.0±10.2% and 49.1%±5.1%, respectively. The highest porosity of PGS/POSS8 scaffolds could be due to the lower viscosity of the mixture of the prepolymer with these particles, and thus a better wetting of the porogen template. In the supplementary content the tomography of PGS/POSS8 can be seen as a video of the cross-section of the scaffold.

Most pores have diameters from 6 to 50 μm in all types of samples, mainly in those with POSS8 particles. The pure PGS and PGS/POSS1 samples have more pores with sizes above 50 μm. In Figure 5, a 3D renderization of the pore size can be observed. The pores are colour-codified according to their size, so their distribution and size throughout the porous cylinder can be observed. In the lower part of the scaffolds there are no pores. This can be due to a hindered diffusion of the viscous pre-polymer through the salt template, leaving a visible bulk part above that has to be necessarily excluded for analyses.

Thermal analysis of POSS particles and the films

Figure 6 displays the mass change as a function of temperature, for the particles and films. It can be observed that the mass loss for POSS1 particles is greater than for POSS8 ones. POSS particles consist of an inorganic part and an organic one, so when the particles are heated up the organic part starts to degrade leaving the inorganic fraction as residue. But POSS1 and POSS8 particles show a very different behaviour: POSS1 particles lose nearly all the mass, whereas POSS8 ones lose just about 50%. Moreover, the temperature interval of the thermal degradation is different in both materials: POSS1 particles start to decompose at 189ºC until 495ºC, with a degradation peak at 322.54ºC, whereas POSS8 ones degrade in the range of 330 to 620ºC with the peak at 540.73ºC. As for the films there are not great differences between samples. For all films the thermal degradation starts about 330ºC and extends up to 550ºC, exhibiting a degradation peak around 430ºC. The only difference is that for the PGS/POSS8 films the mass residue after the ramp is higher than for the other two samples, as expected. This is because the POSS8 particles are more thermo-resistant, as observed in the TGA curves of pure particles. However, it

seems that the incorporation of 5% wt/wt of POSS particles in PGS does not modify its thermal resistance significantly.

Differential scanning calorimetric (DSC) measurements were also performed with the films. In Figure 6C the normalized heat capacity is shown. The kink observed in the range from -40 to -15ºC is the glass transition, as a sloped region in the specific heat. The glass transition temperature (T_g), obtained as the inflection point, is similar for all materials: -23.64ºC for pure PGS films, -20.27ºC for PGS/POSS1 films, and -22.85ºC for PGS/POSS8 films.

Next, an exothermic crystallization peak can be observed, more clearly in the PGS/POSS1 films. In PGS and PGS/POSS8 films, this peak is hardly discernible. Finally, the melting of the crystalline phase can be observed, with its peak at around 6.5ºC for all samples. For PGS/POSS1 films, there is a subsequent smaller melting peak, which seems to be the melting transition of the organic part in the POSS1 particles. This behaviour can be related to the more pronounced crystallization peak of these materials, observed at around -16ºC, partially attributed to the crystallization of the particles' organic chains that melt at higher temperatures (around 36ºC).

The behaviour observed herein for pure PGS films is consistent with previous results of the authors [20] obtained for samples cured at lower temperatures (110 and 120ºC). These less cured samples showed an exothermic peak followed by a melting peak of those chains able to crystallize. This peak tended to get closer to the glass transition to almost vanish for PGS cured at 48 h. However, it has to be taken into consideration that the samples scanned here were not thoroughly rinsed in tetrahydrofuran to remove non-crosslinked macromers as it was done in the previous work, but in ethanol (in which PGS swells less).

Non-crosslinked remnant chains are probably those able to crystallize and melt. As highlighted in the previous work, the total mass fraction of non-crosslinked chains accounts for 6% of the weight of the samples, and its elimination is key to avoid their diffusion to the surrounding medium and eventual adverse reactions.

Density and swelling of the films

The density results obtained for the films were 1.127 ± 0.010 gml^{-1} for pure PGS films, and 1.125 ± 0.001 gml^{-1} and 1.139 ± 0.001 gml^{-1} for PGS/POSS1 and PGS/POSS8 respectively. The statistical assessment of differences indicates that there is a significant difference between the films with POSS8 particles and the other two compositions. The density of POSS1 particles is 1.13 gml^{-1} while for POSS8 it is 1.20 according to Hybrid Plastic Inc., so the densities obtained for the blends fit well those of ideal mixtures of their components.

On the other hand, the swelling capacity of the films was analyzed, in three different media: artificial saliva, deionized water and cell culture medium. The films were weighed after 1, 2, 5, 7 and 12 days. It was observed that the weight increased for the first 48 h, and by the fifth day it become a stable value.

The results at equilibrium are shown in Figure 7. The statistical analysis showes significant differences between the materials only when immersed in water, in particular there is significant difference between PGS films and PGS/POSS1 or PGS/POSS8, *i.e.*, with the addition of any of these particles, the swelling capacity of the hybrids increases. Nanoparticles act probably as imperfections in the percolated PGS network, allowing a greater expansion and water holding.

Mechanical properties

For the scaffolds (Figure 8), the average initial elastic moduli were around 60-70 kPa without any significant difference between compositions and around 220 kPa in the second linear stage. The Young's moduli of the films did increase with the presence of POSS nanoparticles, POSS8 in particular. This result indicates that even POSS1 nanoparticles, with showed melt organic chains at this temperature (Figure 6), can also improve PGS mechanical properties.

The moduli of the films are much higher than those of the scaffolds, as expected. This is because the scaffolds are porous structures, so when a force is applied to the porous material, the trabecular structure starts to support such force, but it progressively collapses reaching a deformation that is related to its porosity. The value obtained here for the PGS film does not agree with that reported in [20], averaged 4638.84 kPa, but those films were well rinsed to eliminate non-crosslinked chains and residues (which amount to 6%), whereas these ones were measured as prepared. In any case, these values are of the order of natural soft tissues [31].

The porosity can be correlated with the mechanical properties of the scaffolds, according to [32]. The so-called reduced modulus of a scaffold, E_R, depends on its porosity, as follows:

$$E_R = E(1-\pi)^2$$

where E is the modulus obtained for the bulk polymer and π is the porosity of the scaffold. Taking the Es obtained for the films (third column in the table) as the moduli of the bulk polymer in each case, the resulting E_R does not represent the measured moduli of the

scaffolds, but higher. Interestingly enough, taking the E_2 moduli of the scaffolds as the moduli of the bulk polymers, the equations fits well the tensile behaviour of the scaffolds, especially for PGS/POSS8 ones, which showed a more uniform architecture and a higher porosity. This finding suggests that curing in the presence of the porogen template yields a PGS network slightly different from that obtained in an empty mould.

Degradation

All porous structures showed to be stable and did not lose their integrity after 4 weeks in artificial saliva or deionized water at pH 6.4. The results of the scaffolds incubated in artificial saliva showed large deviations (except PGS/POSS8), the mass loss being marginal: 1.339±1.127%, 2.126±0.728% and 0.412±0.097% for PGS, PGS/POSS1 and PGS/POSS8 scaffolds, respectively. Nevertheless, it has to be taken into account that artificial saliva contains many dissolved salts that may precipitate on the materials. A rinse with deionized water was imperative at withdrawal before drying the samples, in order to remove most of the salts, but a fraction of them cannot be ruled out.

As for the samples immersed in deionized water, the deviations of the results were smaller, and it was found that PGS/POSS1 and PGS/POSS8 lose more weight, 1.086±0.239% and 0.845±0.173%, respectively, than PGS scaffolds, which lose only 0.487±0.153%. Differences between the hybrid scaffolds and pure PGS ones were found to be statistically significant, and could be due to the fact that hybrid scaffolds swell more than PGS ones, leading to a faster bulk hydrolysis.

Nucleation of hydroxyapatite

After 2 weeks of immersion in artificial saliva (AS), some isolated hydroxyapatite (HAp) formations were observed, and after 4 weeks most of the surfaces were completely coated, showing hemispherical structures sized 1-2 μm typical of HAp structures [33-35], and even aggregates growing from secondary nucleation points. In Figure 9A-C an overall view of the scaffolds' surface is shown. In Figure 9D-E, the crystals that conform these cauliflower-like structures are shown, measuring around 0.1-0.2 μm. On hybrid scaffolds, these structures grow more uniformly throughout the surfaces and their size is more homogeneous.

After 2 weeks, on pure PGS scaffolds crystals nucleate only in specific zones and grow preferentially there. On pure PGS scaffolds, HAp probably nucleate in defects of the surface or zones with different roughness, whereas on hybrid ones silica-based particles can act as imperfections or nucleation points, and since they are well distributed throughout the surface, the new crystallites grow more homogeneously.

Elemental analysis was performed in order to assess the composition of these crystals and confirm that they were bone-like HAp (Figure 9F, as an example). For all the samples tested, the hemispherical structures formed were composed of crystals based on Ca-P, which are the elements present in the hydroxyapatite molecules ($Ca_{10}(PO_4)_6)(OH)_2$) at a ratio of 1.67 [35]. The Ca/P ratio after 4 weeks was in these samples lower, between 1.24 and 1.61, the highest ratio being obtained in PGS/POSS8 scaffolds. However, this ratio has been found to tend to 1.67 in samples incubated in a simulated body fluid [26].

Biocompatibility

In Figure 10 the results of the cell viability test are shown. Cell viability was the lowest in PGS/POSS1 films, which suggests that these particles might be slightly cytotoxic. Pure PGS and PGS/POSS8 showed values around 70% with respect to the positive control, but with a considerable deviation. As noted above, the presence of non-crosslinked PGS macromers and oligomers diffused to the culture medium cannot be excluded, and could account for these results, not as positive as expected based on previous results with neat PGS [20].

As for the scaffolds, cell viability was around 60% in all cases, suggesting that the porosity played a more important role on cellular behaviour than their composition. When the materials have interconnected pores there is much more available surface per volume unit for the cells and a better distribution of nutrients throughout the materials, which facilitates cell adhesion and proliferation [34,36]. However, 48 h was probably a too short period for the cells to colonize these three-dimensional structures. Maybe a longer culture could support this idea, because cells would reach confluence on films much earlier than in scaffolds, where they could proliferate more.

4. CONCLUSIONS

Nanocomposites based on PGS with POSS particles were successfully synthesized as films and sponge-like scaffolds by curing a mixture of the PGS pre-polymer with the nanoloads in the presence of a salt template. The resulting materials were hydrophobic elastomers that did not lose integrity or the nanoloadings during the porogen leaching, which involved several rinsing in affine solvents.

POSS particles were homogeneously distributed throughout the polymer matrices, improved the mechanical properties of the pure elastomer and improved its bioactivity, acting as nucleation points that promote a more uniform growth of hydroxyapatite hemispherical structures. Among both particles studied, POSS8 stand out for its easier manipulability, easier injection of the pre-polymer mixture in the porogen template, better distribution, higher porosity, more bioactive character and better biological performance.

ACKNOWLEDGMENTS

This work was partially funded by the Spanish Ministerio de Economía y Competitividad through DPI2015-65401-C3-2-R project and by the German Research Foundation (DFG/MWK INST 1525/39-1 FUGG). The authors acknowledge Dr. Kirsten Techmer from Geoscience Center of the Georg-August-University Göttingen for performing the EDX-SEM analysis, the assistance and advice of the Jülich Centre for Neutron Science (JCNS) and Institute for Complex Systems (ICS), Forschungszentrum Jülich GmbH (Germany), and the Electron Microscopy Service of the Universitat Politècnica de València (Spain). A.V.-Ll. acknowledges the support of the Generalitat Valenciana, Conselleria de Educación, Investigación, Cultura y Deporte through project AEST/2018/014.

REFERENCES

[1] Wang Y, Ameer GA, Sheppard BJ, Langer R. A tough biodegradable elastomer. Nat Biotechnol 2002;20:602–606.

[2] Loh XJ, Karim AA, Owh C. Poly(glycerol sebacate) biomaterial: synthesis and biomedical applications. J Mater Chem B 2015;3:7641–7652.

[3] Rai R, Tallawi M, Grigore A, Boccaccini AR. Synthesis, properties and biomedical applications of poly(glycerol sebacate) (PGS): A review. Prog Polym Sci 2012;37:1051–1078.

[4] Serrano MC, Chung EJ, Ameer GA. Advances and applications of biodegradable elastomers in regenerative medicine. Adv Funct Mater 2010;20:192–208.

[5] Zhang X, Jia C, Qiao X, Liu T, Sun K. Porous poly(glycerol sebacate) (PGS) elastomer scaffolds for skin tissue engineering. Polym Test 2016;54:118–125.

[6] Chen QZ, Bismarck A, Hansen U, Junaid S, Tran MQ, Harding SE, Ali NN, Boccaccini AR. Characterisation of a soft elastomer poly(glycerol sebacate) designed to match the mechanical properties of myocardial tissue. Biomaterials 2008;29: 47–57.

[7] Salehi S, Fathi M, Javanmard SH, Bahners T, Gutmann JS, Ergün S, Steuhl KP, Fuchsluger TA. Generation of PGS/PCL Blend Nanofibrous Scaffolds Mimicking Corneal Stroma Structure. Macromol Mater Eng 2014;299: 455–469.

[8] Yang K, Zhang J, MA X, Ma Y, Kan C, Man H, Li Y, Yuan Y, Li C. β-Tricalcium phosphate/poly(glycerol sebacate) scaffolds with robust mechanical property for

bone tissue engineering. Mater Sci Eng C 2015;56:37–47.

[9] Lang N, Pereira MJ, Padera R, Wasserman S, Freudenthal F, Ferreira LS. A blood-resistant surgical glue for minimally invasive repair of vessels and heart defects. Sci Transl Med 2015;6: no. 218.

[10] MacDonald RA, Laurenzi BF, Viswanathan G, Ajayan PM, Stegemann JP. Collagen-carbon nanotube composite materials as scaffolds in tissue engineering. J Biomed Mater Res A 2005;74:489–496.

[11] Saito N, Usui Y, Aoki K, Narita N, Shimizu M, Hara K, Ogiwara N, Nakamura K, Ishigaki N, Kato H, Taruta S, Endo M. Carbon nanotubes: biomaterial applications. Chem Soc Rev 2009;38:1897–1903.

[12] Chawla R, Tan A, Ahmed M, Crowley C, Moiemen NS, Cui Z, Butler PE, Seifalian AM. A polyhedral oligomeric silsesquioxane-based bilayered dermal scaffold seeded with adipose tissue-derived stem cells: In vitro assessment of biomechanical properties. J Surg Res 2014;188:361–372.

[13] Campbell K, Craig DQM, McNally T. Poly(ethylene glycol) layered silicate nanocomposites for retarded drug release prepared by hot-melt extrusion. Int J Pharm 2008:363:126–131.

[14] Scott W. Thermal Rearrangement of Branched Chain Methylpolysiloxanes. J Am Chem Soc 1946;68:356–358.

[15] Li GZ, Wang LC, Ni HL, Pittman CU. Polyhedral oligomeric silsesquioxane (POSS) polymers and copolymers: A review. J Inorg Organomet Polym

2001;11:123–154.

[16] Phillips SH, Haddad TS, Tomczak SJ. Developments in nanoscience: Polyhedral oligomeric silsesquioxane (POSS)-polymers. Curr Opin Solid State Mater Sci 2004;8:21–29.

[17] Jungebluth P, Alici E, Baiguera S, Blomberg P, Bozóky B et al. Tracheobronchial transplantation with a stem-cell-seeded bioartificial nanocomposite: A proof-of-concept study. Lancet 2011;378:1997–2004.

[18] Nayyer L, Birchall M, Seifalian AM, Jell G. Design and development of nanocomposite scaffolds for auricular reconstruction. Nanomedicine Nanotechnology Biol Med 2014;10:235–246.

[19] Vilariño-Feltrer G, Muñoz-Santa A, Conejero-García Á, Vallés-Lluch A. The effect of salt fusion processing variables on structural, physicochemical and biological properties of poly(glycerol sebacate) scaffolds. International Journal of Polymeric Materials and Polymeric Biomaterials, submitted ID GPOM-2019-4900.

[20] Conejero-García Á, Rivero Gimeno H, Moreno Sáez Y, Vilariño-Feltrer G, Ortuño-Lizarán I, Vallés-Lluch A. Correlating synthesis parameters with physicochemical properties of poly(glycerol sebacate). Eur Polym J 2017;87:406-419.

[21] Gao J, Crapo M, Wang Y. Macroporous elastomeric scaffolds with extensive micropores for soft tissue engineering. Tissue Eng 2006;12:917-925.

[22] Klimek J, Hellwig E, Ahrens G. Fluoride taken up by plaque, by the underlying enamel and by clean enamel from three fluoride compounds in vitro. Caries Res 1982;16:156–161.[23] Zhao X, Wu Y, Du Y, Chen X, Lei B, Xue Y, Ma PX. A highly bioactive and biodegradable poly(glycerol sebacate)–silica glass hybrid elastomer with tailored mechanical properties for bone tissue regeneration. J Mater Chem B 2015;3:3222

[24] Wu Y, Shi R, Chen D, Zhang L, Tian W. Nanosilica Filled Poly(glycerol-sebacate-citrate) Elastomers with Improved Mechanical Properties, Adjustable Degradability, and Better Biocompatibility. J Appl Polym Sci 2012;123:1612–1620.

[25] Liang SL, Cook WD, Thouas GA, Chen QZ. The mechanical characteristics and in vitro biocompatibility of poly(glycerol sebacate)-Bioglass® elastomeric composites. Biomaterials 2010;31:8516e8529.

[26] Kokubo T, Takadama H. How useful is SBF in predicting in vivo bone bioactivity? Biomaterials 2006;27:2907–2915.

[27] Socrates G. Organic Silicon Compounds. In: Infrared and Raman characteristic Group Frequencies: Tables and Charts., 3rd ed., John Wiley & Sons, Inc., 2001.

[28] Wahab MA, Kim I, Ha CS. Microstructure and properties of polyimide/poly(vinylsilsesquioxane) hybrid composite films. Polymer 2003;44:4705-4713.

[29] Song XY, Geng HP, Li QF. The synthesis and characterization of polystyrene/magnetic polyhedral oligomeric silsesquioxane (POSS)

nanocomposites. Polymer 2006;47:3049-3056.

[30] Kerativitayanan P, Gaharwar AK. Elastomeric and mechanically stiff nanocomposites from poly(glycerol sebacate) and bioactive nanosilicates. Acta Biomater 2015;26:34–44.

[31] Liu J, Zheng H, Poh PSP, Machens HG, Schilling AF. Hydrogels for engineering of perfusable vascular scaffolds.

[32] Gibson LJ, Ashby MF. Cellular solids: Structure and Properties, Cambridge University Press: Cambridge, 1997, p. 186.

[33] Vallés Lluch A, Gallego Ferrer G, Monleón Pradas M. Biomimetic apatite coating on P(EMA-co-HEA)/SiO2 hybrid nanocomposites. Polymer 2009; 50(13): 2874-2884.

[34] Jones JR. Scaffolds for Cell and Tissue Engineering. In: Wiley Encyclopedia of Biomedical Engineering, John Wiley & Sons, Inc., 2006.

[35] Suárez-González D, Barnhart K, Saito E, Vanderby R, Hollister S, Murphy WL. Controlled nucleation of hydroxyapatite on alginate scaffolds for stem cell-based tissue engineering. J Biomed Mater Res 2010;95:222–234.

[36] Dhandayuthapani B, Yoshida Y, Maekawa T, Kumar DS. Polymeric scaffolds in tissue engineering application: A review. Int J Polym Sci 2011;2011:Article ID 290602.

Figures

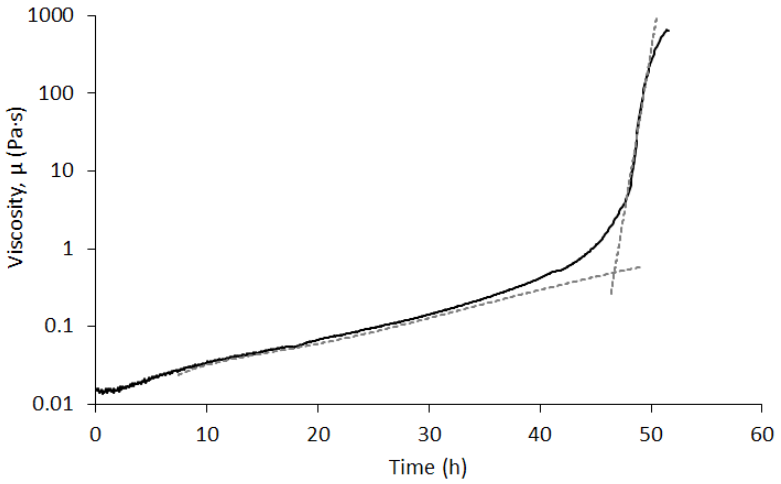

Figure 1. Viscosity curve as PGS polymerizes and crosslinks yielding a percolated network, shown as the viscosity vs. time (−), and hypothetical viscosity extrapolation in the pre-polymerization and curing stages (- -).

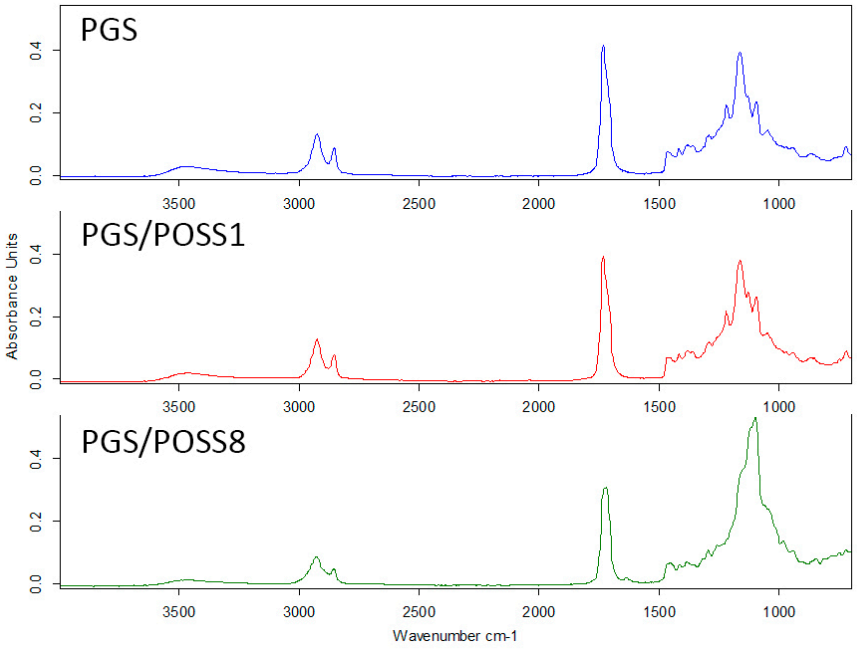

Figure 2. Infrared spectra for PGS, PGS/POSS1 and PGS/POSS8 films.

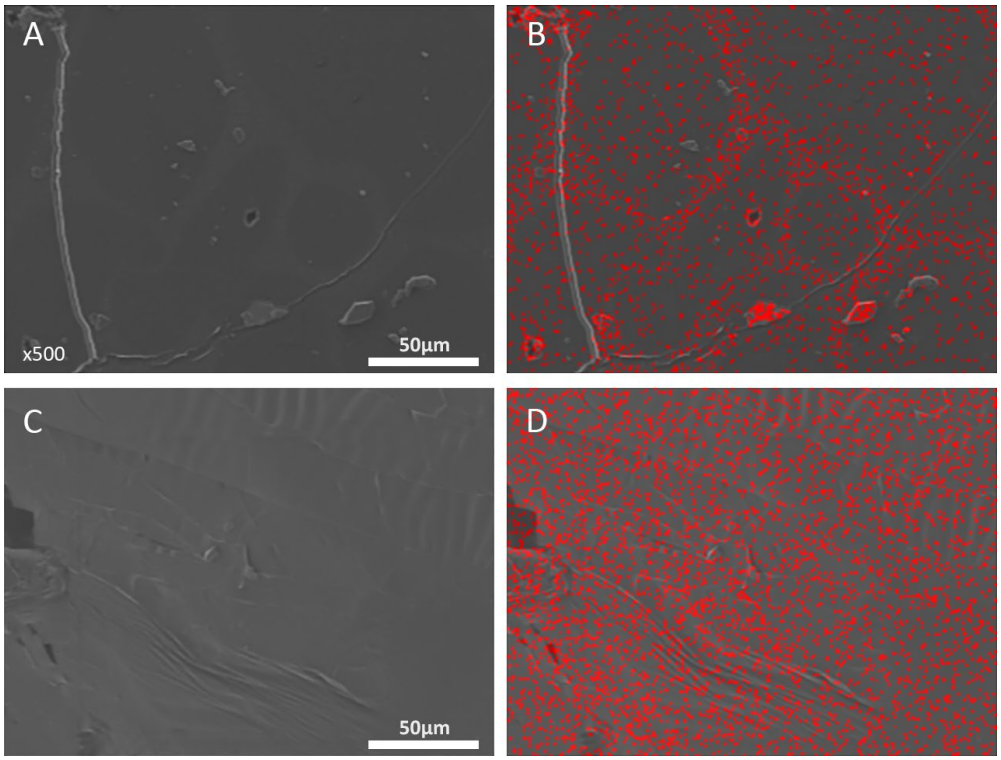

Figure 3. Surface FESEM images of PGS/POSS1 film (A) and PGS/POSS8 (C), and same images with EDS silicon lectures in red (B and D, respectively). Scale bar: 50 µm.

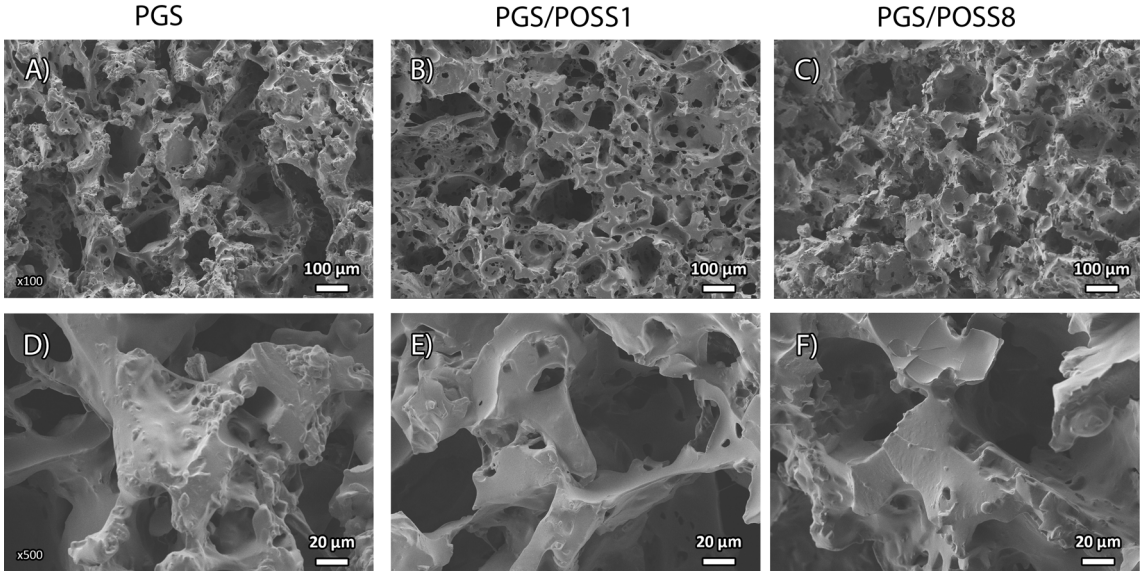

Figure 4. FESEM images of the hybrid scaffolds.

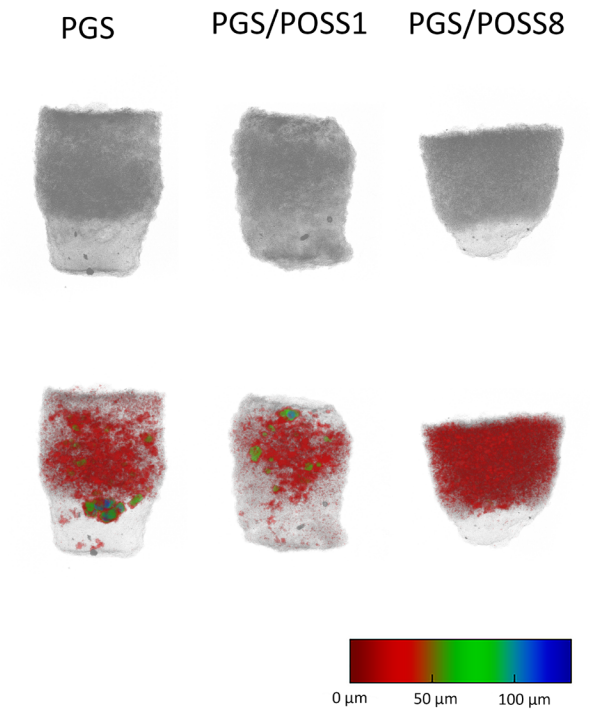

Figure 5. Color-coded pore size and its distribution throughout the cylindrical scaffolds (before slicing), obtained by MicroCT.

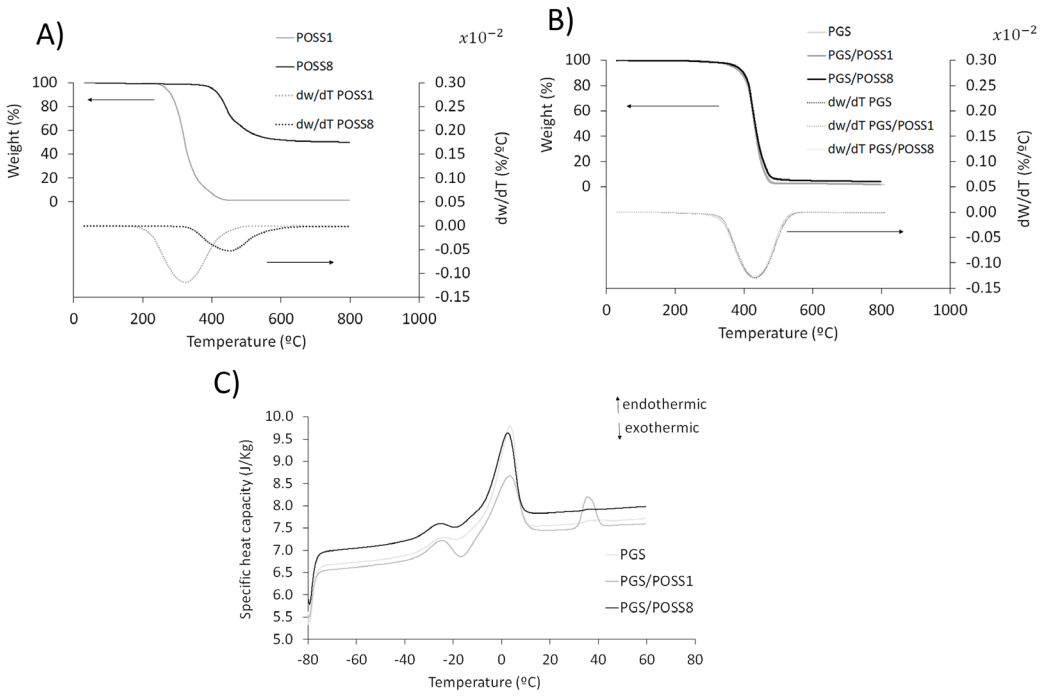

Figure 6. Weight loss vs. temperature of POSS1 and POSS8 particles (A), PGS, PGS/POSS1 and PGS/POSS8 films (B), and normalized heat flow as a function of temperature for PGS, PGS/POSS1 and PGS/POSS8 samples (C).

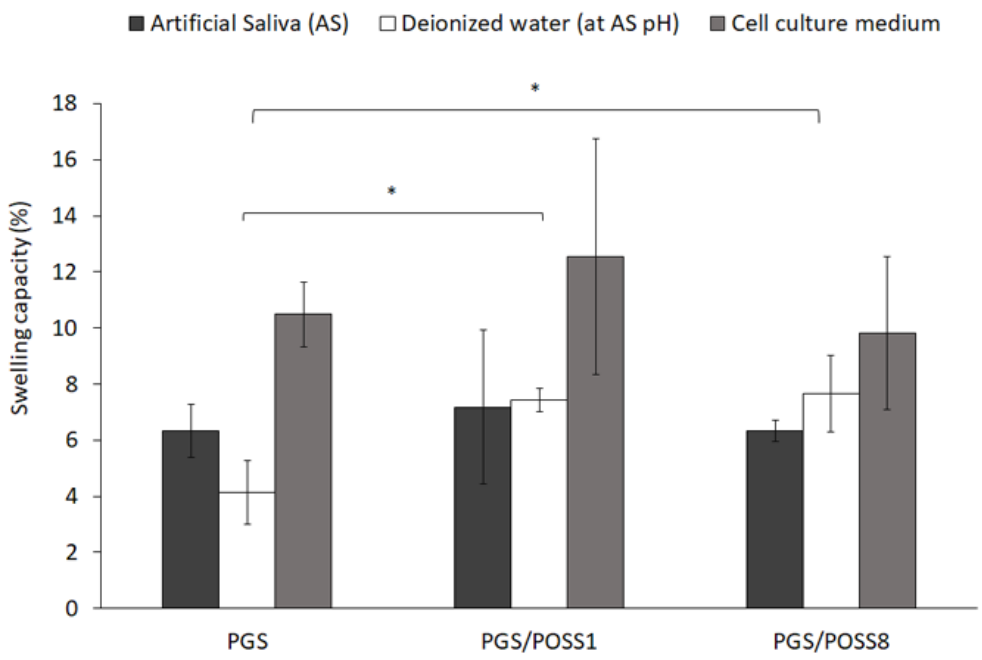

Figure 7. Swelling capacity for PGS, PGS/POSS1 and PGS/POSS8 films in the three different media of the legend. Differences are statistically significant between pairs marked with (*).

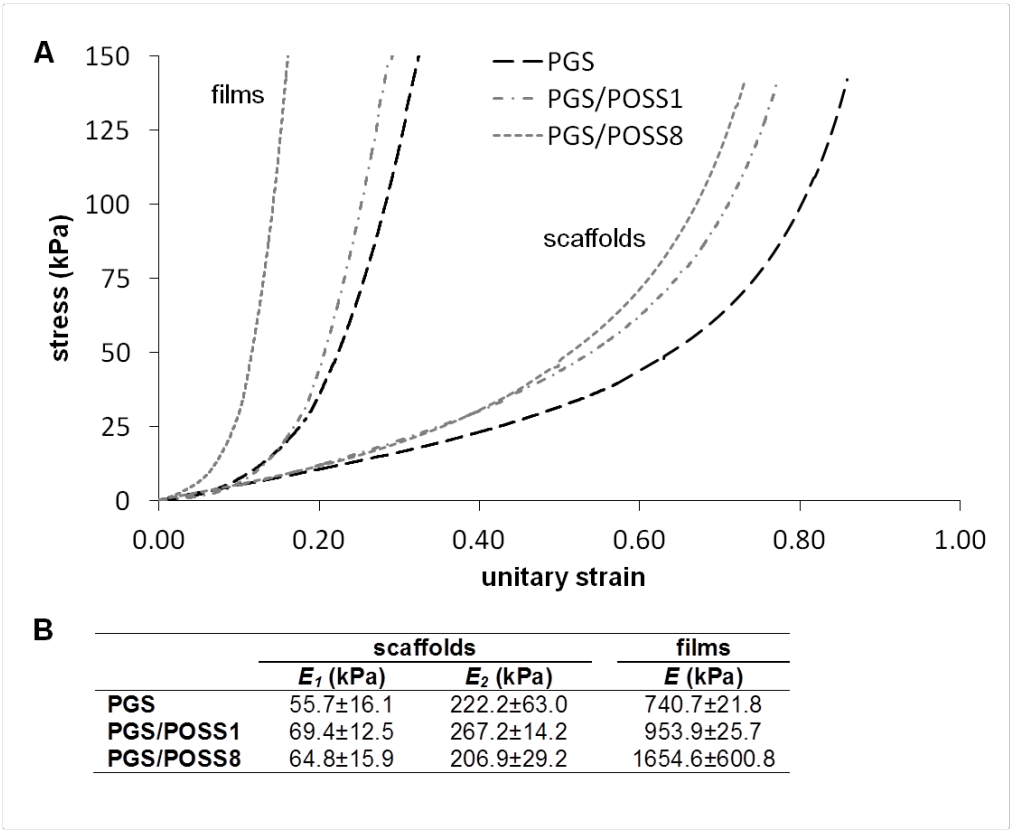

B

	scaffolds		films
	E_1 (kPa)	E_2 (kPa)	E (kPa)
PGS	55.7±16.1	222.2±63.0	740.7±21.8
PGS/POSS1	69.4±12.5	267.2±14.2	953.9±25.7
PGS/POSS8	64.8±15.9	206.9±29.2	1654.6±600.8

Figure 8. Stress-strain curves for films and scaffolds (A) and Young moduli (B).

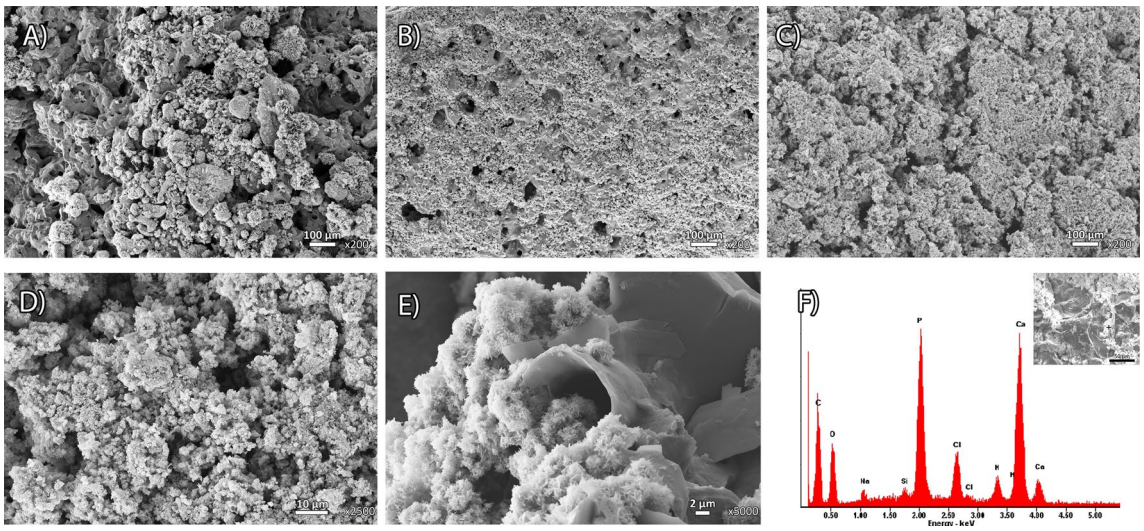

Figure 9. FESEM images of the surface of PGS (A), PGS/POSS1 (B) and PGS/POSS8 (C) scaffolds after immersion in AS for 2 weeks. Detail of the crystalline formations on

PGS/POSS1 after 4 weeks (D) and PGS/POSS8 (E). EDS spectra of PGS/POSS8 after 3 weeks in AS (F).

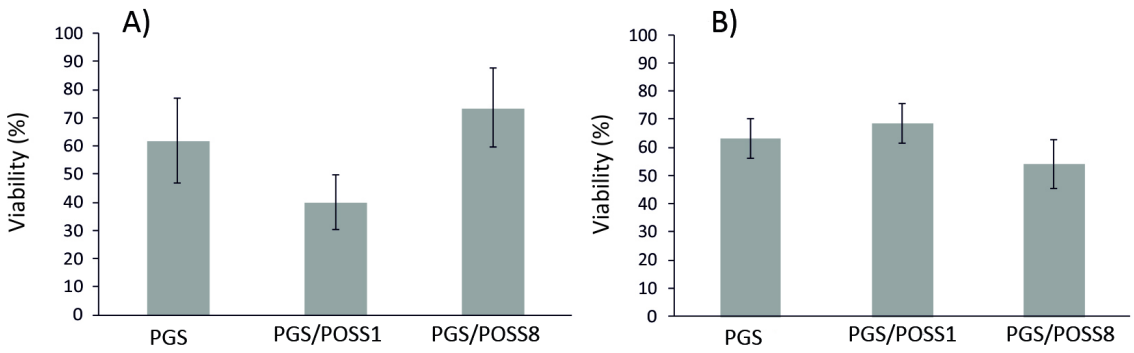

Figure 10. Cell viability results for films (A) and scaffolds (B).